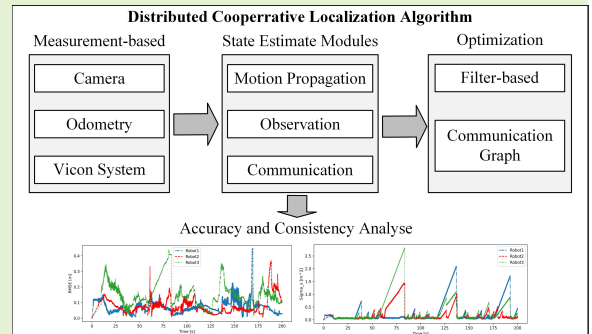


Robust and Convergent Distributed Cooperative Localization with Labelled Bernoulli Random Finite Set

Hongmei Chen, Haifeng Wang, and Wen Ye, *Member, IEEE*, Dongbing Gu, *Senior, IEEE*

Abstract—Cooperative localization is critical for multi-robot systems to accurately ascertain their positions in the environment. This paper presents a robust and convergent distributed cooperative localization algorithm to effectively address localization inaccuracies and inconsistency caused by intermittent or limited absolute observation capabilities. The algorithm integrates three key modules: propagation, observation, and communication, enabling each robot to estimate its states and measure noise covariance simultaneously. To enhance the estimation consistency, inter-vehicle relative observations and landmark absolute observations are modeled as multi-Bernoulli random finite sets (RFSs), with robot states updated using a coupled correlation scheme. By combining extended particle filtering, and covariance intersection techniques, the algorithm efficiently handles intermittent observations, leading to substantial improvements in localization accuracy and estimation consistency. Further, the proofs of convergent consistency are provided in the paper, validating the algorithm's robustness and convergence.

Index Terms—Cooperative localization, multi-robot systems, labelled Bernoulli random finite set, communication.



I. INTRODUCTION

MULTI-ROBOT Cooperative Localization (CL) has emerged as a pivotal research area within the domain of modern intelligent robots and autonomous systems. It has garnered increasing attention from researchers due to its broad applicability in various fields, including search and rescue [1], [2], [3], warehousing [4], [5], [6], and military applications [7], [8]. In practical scenarios, multiple robots must collaborate and communicate with one another to effectively navigate and accomplish tasks collectively. In scenarios where no observations or only intermittent observations are available within the environment, robotic systems could face challenges

This work was supported in part by the National Key RD Program of China under Grant 2023YFC2205603, the National Natural Science Foundation of China under Grant U1804161, Grant 61901431, the Basic Research of National Institute of Metrology under Grant AKYJJ1906, the Henan science and technology research under Grant 222102210269, the Haizhi project of Henan Association for science and technology under Grant HZ202201, the cultivation plan of young teachers of Henan University of Technology under Grant 21420169, the innovation fund of Henan University of Technology under Grant 2021zkcj07.

Hongmei Chen is with Henan University of Technology, Zhengzhou, 450000, China (e-mail: chenhongmei@haut.edu.cn). Currently, She is an academic visitor at University of Essex.

Haifeng Wang is with Henan University of Technology, Zhengzhou, 450000, China (e-mail: wanghaifeng@stu.haut.edu.cn).

Wen ye, is with Institute of Mechanics and Acoustics Metrology, National Institute of Metrology, Beijing, 102200, China e-mail: wenyeb@buaa.edu.cn).

Dongbing Gu is with School of Computer Science and Electronic Engineering, University of Essex, CO4 3SQ, Colchester, UK (e-mail: dgu@essex.ac.uk).

in acquiring accurate absolute positional information. This could result in information gaps during the navigation process. Additionally, limited collaboration among the robots could give rise to redundant information and repeated computations, thereby impacting the overall accuracy and consistency of navigation algorithms. Therefore, it is of significant research importance and practical value to address the challenges associated with collaborative multi-robot localization in complex environments.

Researchers have applied a collaborative approach for multi-robot localization, which involves fusing data from on-body and external sensors, as well as utilizing wireless communications. Centralized cooperative localization (CCL) achieved success in some tasks but suffers from single point failures and/or heavy communication overheads [9], [10], [11], [12], [13], [14], [15], [16]. In contrast, Distributed Collaborative Localization (DCL) [17], [18], [19], [20], [21], [22] adopted a decentralized algorithm to improve reliability, real-time performance, and reduce communication costs, making it suitable for large-scale multi-robot navigation tasks.

DCL approaches face positioning accuracy and consistency challenges. To address these challenges, controlling the estimate correlation through data flow management has been explored. Leung et al. [23] proposed an information transfer scheme that allows distributed robots to obtain latency estimates comparable to centralized robots but requires a large amount of communication due to data relaying. Su et al. [24] introduced a new information exchange mechanism using

entropy for confidence probability computation, which could reduce unnecessary exchanges but rely heavily on synchronisation, potentially increasing pose estimation uncertainty. Bailey et al. [25] proposed a state-exchange-based approach, sharing independent estimates within the vehicle network to mitigate the over-convergence risk. However, it has drawbacks: limited benefit beyond visible neighbors and increased computational overhead.

Covariance intersection (CI), an estimation method, addressed the inconsistent state estimation problem in distributed cooperative localization [21]. It enables the vehicles to maintain a group state estimate and share it with neighbors for consistency. Zhu et al. [26] mentioned that estimating the cross-correlation reduces the computation of redundant information. However, CI and cross-correlation estimation suffer from reduced accuracy due to observation noise variance expansion [19], [27], [28]. Estimation-based approaches offer advantages: over-convergence risk is eliminated, and low communication demands avoid extensive information relay. Chang et al. [29] introduced Global State–Covariance Intersection (GS-CI) by combining the state exchange and estimation-based ideas to achieve accuracy comparable to centralized methods. Nonetheless, GS-CI’s performance could be deteriorated in constrained observation scenarios, affecting estimation accuracy and consistency.

In brief, existing research has extensively explored multi-robot navigation algorithms. However, the accuracy of positioning and the convergence consistency of distributed CL algorithms, particularly in intermittent measurement environments, still pose significant challenges. This study aims to address some of these research challenges and develop a more robust and reliable multi-robot CL system through four specific objectives. Firstly, a novel algorithm titled “Labeled Multi-Bernoulli on Global State by Extended Particle Filter (LMB-GS-EPF)” is designed. This algorithm seamlessly integrates three distinct state updating strategies: propagation, observation, and communication. This contributes to the simultaneous estimation of robot position and measurement noise covariance, ultimately enhancing overall positioning accuracy. Secondly, Random Finite Set (RFS) and Labeled Multi-Bernoulli (LMB) of particles are employed to take the correlation between observations into consideration and incorporate more historical information into the observation updating process. This innovation significantly enhances the algorithm’s ability to associate and integrate diverse observation data, thereby bolstering its robustness. Furthermore, advanced techniques including extended particle filtering and CI are leveraged for precise state estimation and probabilistic correlation. These steps collectively improve the algorithm’s overall accuracy and reliability. Lastly, meticulous design of communication topology and strategy coefficient allocation ensures effective information exchange among robots. This final phase not only encompasses the comprehensive multi-robot cooperative localization algorithm but also rigorously proves its convergence consistency, further affirming its robustness and effectiveness.

This paper is structured as follows: section II reviews related work on cooperative navigation, focusing on RFS and LMB

techniques. In section III, we offer an overview of Cooperative Localization (CL) modeling for multi-robot systems, emphasizing explicit communication. section IV details the integrated observation update strategy employing the LMB filters. The design of communication topology and coefficient assignments for the update strategy, along with the proof of algorithm convergence consistency, is presented in section V. Experimental results and algorithm analysis are discussed in section VI. Finally, section VII provides a conclusion and future work.

II. RELATED WORK

RFS is a probabilistic framework widely applied in modeling and handling situations with uncertain and dynamically changing target quantities, particularly in the domains of multi-robot systems and sensor fusion. In [30], RFS is employed to model the birth/death of targets, extending the Probability Hypothesis Density (PHD) filter for recursive propagation of tracking density for environmental detection and targets. However, limitations arise when dealing with uncertain dynamic targets and limited sensor ranges. [31] successfully reduces false negatives and false positives in target detection with limited sensor visibility, enabling a robot swarm to effectively track the targets. Meanwhile, [32] introduces a Rao-Blackwellized labeled multi-Bernoulli SLAM (LMB-SLAM) filter and utilizes Gaussian mixture LMB filters for MAP estimation, thereby obtaining a more accurate map and improving single-vehicle trajectory estimation. In contrast, [33] discusses full-distributed multi-robot simultaneous localization and mapping (SLAM), where maps of multiple robots are updated using RFS and PHD. However, this approach neglects the uncertainty in data association, resulting in decreased localization performance. To mitigate this issue, the covariance intersection (CI) technique is employed to consider the correlation between target states, and improve the accuracy.

In addressing dynamic estimation and convergence issues for multiple vehicles, [34] employs RFS and PHD filtering for dynamic estimation of multi-vehicle states, and [35] proposes two approximation strategies to address constraints in GCI fusion. However, these methods inadequately consider the system consistency during information exchange and fusion among sensors. [36] employs RFS theory to propose decision and control algorithms, enabling collaborative work among agent teams in handling randomly appearing and disappearing targets in a surveillance area. [37] introduces RFS concepts, proposing a joint spatial registration and state estimation solution to enhance positioning accuracy, yet still faces communication and computation challenges in collaborative multi-vehicle localization. [38] applies the ICI algorithm and introduces a distributed particle filter that optimizes the entire network iteratively. This approach ensures the asymptotic consistency in target tracking. Additionally, [39] introduces LMB to provide a more flexible modeling approach without the need for high signal-to-noise ratio for formal trajectory estimation. [40] proposes a fast implementation method for the LMB filter based on joint prediction and update, converting the predicted LMB distribution into its corresponding δ -GLMB

representation. However, the LMB filter incurs higher computational costs, especially in scenarios with a high number of measurements, exhibiting cubic growth in computation costs.

Several studies have addressed the challenges of communication and computation burdens. [41] presents an innovative approach that significantly reduces these costs by employing strongly weighted Gaussian component sharing and spatial merging of neighboring sensors. [42] introduces an efficient distributed fusion algorithm for sensor networks, which utilizes GCI fusion rules and reduces computation and memory requirements through approximation techniques and fast clustering algorithms. To mitigate computation and communication costs, [43] adopts a centralized Kalman filter estimator distributed into a dimensionality reduction filter. In [44], a parallelized fusion approach for the GCI-GMB fusion posterior effectively reduces computation and memory costs in target tracking tasks by discarding negligibly weighted assumptions. However, this approach lacks an investigation into the estimation of consistency issues that may arise when implementing the algorithm in distributed sensor networks. Furthermore, [45] addresses the multidimensional assignment problem with the multi-sensor generalized labeled multi-Bernoulli (GLMB) filter, while [46] resolves the labeled random finite set (LRFS) density fusion problem using the minimum information loss criterion and introduces the cost rank allocation optimization (RAO) to address the label mismatch (LM) issues between LRFS densities. [47] designs a recursive distributed fusion estimator (DFE) that achieves local state estimation through covariance intersection fusion criteria and transmits local estimates to a remote fusion center (FC) via a communication network, providing convenience for multi-sensor interaction fusion estimates. In [48], a network architecture introduces point-to-point communication among robots and interaction with a central server for information exchange and sharing. Although the algorithm mitigates the effect of sensor noise on localization accuracy through information sharing, state updates in communication mode still play a supplementary role. For intermittent measurement environments, designing a parallelized communication update strategy and topology is crucial for improving the overall localization performance of multi-robot systems.

In summary, RFS technique and LMB filters in multi-robot collaborative localization achieve efficient data fusion for target identification and collaborative localization. However, there is a lack of research on high-precision localization and communication architecture for large-scale robot groups in intermittent measurement environments.

III. BACKGROUND

This section briefly reviews the multi-robot state update model required for this paper, including the motion model, observation model and communication model, and briefly describes the CL algorithm used for GS-CI [29].

A. Motion and Observation Models

We consider the scenarios where multiple robots interact with landmarks with known positional information in a two-

dimensional plane. Each robot is equipped with both proprioceptive and exteroceptive sensors: an odometer for self-motion measurement and a camera for collecting measurements to landmarks or measurements between robots. The index set of the multi-robot system is denoted as $\Omega = \{1, 2, \dots, M\}$, and the set of landmarks as Δ , resulting in $\Omega^* = \Omega \cup \Delta$. At any given time t , the state of robot i is represented by the vector $\mathbb{S}_t^i = [x_t^i, y_t^i, \theta_t^i]^T$. Consequently, the state of the system is denoted by $\mathbb{S}_t = [\mathbb{S}_t^1, \dots, \mathbb{S}_t^M]^T$.

The robot's motion model is established based on the odometer to describe its spatio-temporal displacement. The odometer sensor is classified as a proprioceptive sensor, providing measurements of the robot's linear velocity v_t^i and angular velocity ω_t^i . Let Δt be the time interval between two consecutive motion updates. The discrete motion propagating model for robot i is represented as follows.

$$\mathbb{S}_{t+1}^i = \mathbf{f}_i(\mathbb{S}_t^i, v_t^i, \omega_t^i) = \begin{bmatrix} x_t^i + v_t^i \Delta t \cos(\theta_t^i) \\ y_t^i + v_t^i \Delta t \sin(\theta_t^i) \\ \theta_t^i + \omega_t^i \Delta t \end{bmatrix} \quad (1)$$

where $\mathbb{S}_t^i = [x_t^i, y_t^i, \theta_t^i]^T$, $[x_t^i, y_t^i]^T$ denotes the position of robot i in the absolute coordinate system, and θ_t^i denotes the orientation of robot i at time t .

The observation model describes the relative position of object j as observed by robot i . Therefore, the observation model for robot i can be represented as follows.

$$\mathbf{o}^{ij} = \mathbf{C}^T(\theta_t^i) \left(\begin{bmatrix} x_t^j \\ y_t^j \end{bmatrix} - \begin{bmatrix} x_t^i \\ y_t^i \end{bmatrix} \right) = \mathbf{C}^T(\theta_t^i) \mathbf{H}^{ij} \mathbb{S}_t \quad (2)$$

where \mathbf{C} is the rotation matrix containing the angle parameter θ . It is worth noting that the observation model j contains the observation of robot i on the robot j or landmark Δ . The \mathbf{H} is calculated based on the relative observation information of the robot, as follows.

When robot i observes another robot j , \mathbf{H}^{ij} is denoted as:

$$\mathbf{H}^{ij} = \begin{bmatrix} 0_{2 \times 2} \cdots \underbrace{-I_2}_i \cdots \underbrace{I_2}_j \cdots 0_{2 \times 2} \end{bmatrix}_{2 \times 2N} \quad (3)$$

where I_2 denotes a 2×2 unit matrix. If observation j is a landmark, \mathbf{H}^{ij} is denoted as:

$$\mathbf{H}^{ij} = \begin{bmatrix} 0_{2 \times 2} \cdots \underbrace{-I_2}_i \cdots 0_{2 \times 2} \end{bmatrix}_{2 \times 2N} \quad (4)$$

In this paper, the observation process is carried out by an external camera sensor. The relevant observed variables include the relative distance d^{ij} and the relative attitude ϕ^{ij} . Consequently, the observation of the relative spatial position between robot i and object j is expressed as follows.

$$\mathbf{o}^{ij} = d^{ij} \begin{bmatrix} \cos(\phi^{ij}) \\ \sin(\phi^{ij}) \end{bmatrix} \quad (5)$$

B. Communication Model

In a system comprising M robots, we introduce the concept of a communication directed graph denoted as $G_t^c = (\Omega, E_t^c)$, where Ω represents the set of robots, and $E_t^c \subseteq \Omega \times \Omega$ is the

set of edges representing their communication links between the robots at time t . When robot i receives a message from robot j at time t , it signifies the existence of a directed edge $(j, i) \in E_t^c$. It is worth noting that we assume the presence of self-looping edges $(i, i) \in E_t^c, \forall i \in \Omega$, implying that each robot can utilize its own information. At time t , the communicating neighbor set of robot i is defined as $\mathcal{N}_t^{c,i} = \{l \mid (l, i) \in E_t^c, \forall l \neq i, l \in \Omega\}$. Subsequently, the inclusive communicating neighbor set of robot i is $\mathcal{I}_t^{c,i} = \mathcal{N}_t^{c,i} \cup \{i\}$. Similarly, we define a directed sensing graph denoted as $G_t^s = (\Omega, E_t^s)$ to describe the robot-to-robot measurements, where $E_t^s \subseteq \Omega \times \Omega$ denotes the set of edges, indicating the detection links between robots at time t . If robot i detects robot j at time t , it implies the presence of a directed edge $(j, i) \in E_t^s$. At time t , we define the set of robots detected by robot i as $\mathcal{N}_t^{s,i} = \{l \mid (l, i) \in E_t^s, \forall l \neq i, l \in \Omega\}$, i.e., the set of other robots that robot i detects. We consider that for each robot, the communication radius is greater than the sensing radius of all robots. This setting allows the robots to share information within their communication range, thereby facilitating collaboration among multiple robots.

C. Cooperative Localization Algorithm

The GS-CI [29] localization algorithm employs the EKF framework. We denote the state estimate of each robot i as $\hat{\mathbf{S}}_t^i$ and its corresponding covariance as Σ_t^i .

1) *Motion Propagation Update*: For robot i , the covariance update during the motion propagation process is as follows.

$$\Sigma_{t+1}^i = \Sigma_t^i + \Sigma^{qi} = \Sigma_t^i + \text{Diag}(\Sigma^{u1}, \dots, \Sigma^{uM}) \quad (6)$$

where Σ_t^i represents the state covariance at time t , Σ^{qi} is determined by the input noise, which is the diagonal matrix of Σ^{ui} and depends on the availability of information from neighboring robots.

For robot i , the linear velocity input v_t^i is disturbed by a zero-mean Gaussian random variable \mathbf{n}_v , with a covariance of $\sigma_{n_v}^2$. Linearizing equation (1) [49], which no longer takes into account the estimation of θ , but is continuously given by the on-board odometer, the error propagation equation for robot i itself is

$$\hat{\mathbf{S}}_{t+1}^i \approx \begin{bmatrix} \hat{x}_t^i \\ \hat{y}_t^i \end{bmatrix} + \Delta t \begin{bmatrix} \cos(\theta_t^i) & -v_i \sin(\theta_t^i) \\ \sin(\theta_t^i) & v_i \cos(\theta_t^i) \end{bmatrix} \begin{bmatrix} \mathbf{n}_v \\ \tilde{\theta}_t^i \end{bmatrix} \quad (7)$$

where the orientation estimation error model $\tilde{\theta}_t^i = \theta_t^i - \hat{\theta}_t^i$ comprises a zero-mean Gaussian random variable, with Gaussian variance denoted as $\sigma_{\tilde{\theta}_t^i}^2 = E[(\tilde{\theta}_t^i)^2]$ bounded by $\sigma_{\hat{\theta}_t^i}^2$ which is the given variance. The covariance matrix increment can be expressed as follows.

$$\Sigma^{ui} = (\Delta t)^2 C(\theta_t^i) \begin{bmatrix} \sigma_{n_v}^2 & 0 \\ 0 & v_i^2 \sigma_{\tilde{\theta}_t^i}^2 \end{bmatrix} C^T(\theta_t^i) \quad (8)$$

2) *Observation Update*: The observation update is based on measurements \mathbf{o}^{ij} from the camera, following the standard EKF procedure. With reference to equation (2), the estimated observation error $\tilde{\mathbf{o}}^{ij} = \mathbf{o}^{ij} - \hat{\mathbf{o}}^{ij}$ can be approximated as

$$\tilde{\mathbf{o}}^{ij} \approx \mathbf{H}^{\mathbf{o}^{ij}} \tilde{\mathbf{S}} + C^T(\hat{\theta}_t^i) \mathbf{H}^{ij} \tilde{\mathbf{S}}_t^i - \tilde{\theta}^i + \mathbf{n}_{\mathbf{o}^{ij}} \quad (9)$$

This approximation distinguishes two uncorrelated error terms: the state estimation error $\tilde{\mathbf{S}}$ and the measurement noise $\mathbf{n}_{\mathbf{o}^{ij}}$, where $\mathbf{H}^{\mathbf{o}^{ij}} = C^T(\theta^i) \mathbf{H}^{ij}$. When the observation result \mathbf{o}^{ij} is obtained from the camera, the covariance matrix $\mathbf{R}_{\mathbf{o}^{ij}}$ of $\mathbf{n}_{\mathbf{o}^{ij}}$ can be expressed as

$$\mathbf{R}_{\mathbf{o}^{ij}} = C(\phi^{ij}) \text{diag} \left(\sigma_{d^{ij}}^2, (d^{ij})^2 \sigma_{\phi^i}^2 \right) C^T(\phi^{ij}) \quad (10)$$

The overall covariance update can be represented as

$$(\Sigma_{t+1}^i)^{-1} = (\Sigma_t^i)^{-1} + (\mathbf{H}^i)^T C(\theta_t^i) \mathbf{R}_{\mathbf{o}^{ij}}^{-1} C^T(\theta_t^i) \mathbf{H}^i \quad (11)$$

3) *Communication Update*: In the communication update, robot i utilizes CI [21] to update its estimated information based on external information received from other robots. This process involves incorporating the information sent by robot k to robot i . The covariance update in the reference baseline [29], where only robot k provides information to robot i , can be represented as follows.

$$(\Sigma_{t+1}^i)^{-1} = \beta (\Sigma_t^i)^{-1} + (1 - \beta) (\Sigma_t^k)^{-1}, \beta \in (0, 1) \quad (12)$$

The coefficient value β is determined by minimizing $\det(\Sigma_{t+1}^i)$ or $\text{tr}(\Sigma_{t+1}^i)$ during the estimation fusion process. As β increases, the own estimates for robot i gain more significance in the fusion process.

4) *Problem Statement*: In this paper, we explore the GS-CI baseline algorithm, which consists of three key components: motion propagation, observation updates, and communication updates. While existing algorithms update localization estimates independently through observation and communication, the GS-CI baseline algorithm separates communication from observation, considering communication imperfections due to intermittent or limited observation capabilities. However, this reliance on an one-way chain communication topology in the baseline algorithm introduces limitations, resulting in biased and inconsistent localization results. We also identify potential issues associated with this communication topology. This research aims to address these limitations and enhance localization accuracy and consistency.

The GS-CI algorithm's limited assumption of robot k transmitting information to robot i can hinder communication adequacy. Consequently, it yields suboptimal performance in CL accuracy and estimation consistency. To address this issue, our paper focuses on integrating historical correlation data into the observation update process while optimizing the communication framework, thereby improving estimation consistency. This enhancement serves as the primary motivation behind our research.

IV. METHODS

A. Design Idea of the Proposed Method

To improve the CL accuracy and estimation consistency, we propose a new algorithm, called LMB-GS-EPF algorithm. Firstly, this new algorithm introduces a labeled multi-Bernoulli filter to consider the correlation between observations and incorporate more historical information into the observation updating process. Secondly, we utilize a particle filter to overcome the limitations of EKF algorithm since the system is nonlinear. In addition, we optimize the communication update

part by creating a richer communication structure that allows information exchange between multiple robots, thus improving the accuracy of localization and consistency of estimation. With these improvements, we aim to effectively achieve more robust and accurate cooperative localization.

B. Multi-Labelled Bernoulli Coupled Observation Update

1) *Labelled multi-Bernoulli (LMB) and random finite sets (RFS)*: To represent the state estimates of robots in a multi-robot motion platform, our RFS for the multi-robot motion platform is defined as follows.

$$\mathbf{X}_t = \{x_t^{1,\ell^1}, \dots, x_t^{n,\ell^n}\} \quad (13)$$

where each element x^{n,ℓ^n} is on the space $\mathbb{R} \times \mathbb{L}$ where \mathbb{R} and \mathbb{L} denote the state space and the labeled discrete space, respectively, and $x \in \mathbb{R}$, $\ell \in \mathbb{L}$. Similarly, the finite set of absolute and relative observations for a multi-robot platform can be defined as follows:

$$\mathbf{o}_t^* = \{o_t^1, \dots, o_t^{\Omega^*}\} \quad (14)$$

where * represents the observation set of random collaborative robots in network, each observation component is $o_t^{\Omega^*} \in \mathbb{R}$, where \mathbb{R} represents a vector field, and Ω^* represents the index value of the observed neighbor or landmark.

Bernoulli RFS represents uncertainty about the existence of a single object in a straightforward way. The parameter r represents the probability of the existence of a robot, $s(x)$ represents the state matrix of multiple robots, which is abbreviated as s below; the probability that X is an empty set is $1 - r$. The prior distribution of LMB-RFS is given as

$$\pi(X) = \begin{cases} 1 - r^\ell, & X = \emptyset \\ r^\ell \times s^\ell(x), & X = \{x^1, \dots, x^M\} \end{cases} \quad (15)$$

where X is the union of M independent multi-Bernoulli random finite sets X^i , for example, $X = \cup_{i=1}^M X^i$. A multi-Bernoulli RFS is defined by a parameter set $\{r^i, s^i\}_{i=1}^M$. The LMB-RFS with state space X and label space \mathbb{L} is given by parameter set $\pi = \{r^\ell, s^\ell\}_{\ell \in \mathbb{L}}$.

The RFS representing a multi-robot label in a non-fixed collaborative robot network can be denoted as follows.

$$X_t^* = \{(r_t^\ell, s^\ell(x_t^1)), \dots, (r_t^\ell, s^\ell(x_t^{n_t}))\}, \ell \in L_t^* \quad (16)$$

where X_T^* contains the LMB-RFS component information of multiple robots, r denotes the existence probability, and s denotes the state of a single object, and * is the mark of the random collaborative robot network. s denotes the state of a single object and is marked \mathbb{S} in equation (1).

2) *Particle filter*: In order to establish a reliable prior value for LMB, we use extended Kalman filter (EKF) as the initial calibration value of our particle filter algorithm (PF). Through the use of the PF-EKF algorithm [50], we are able to acquire the initial optimized state \hat{s}_{t+1}^i and covariance $\hat{\Sigma}_{t+1}^i$ of robot i . The optimized state significantly reduces the uncertainty in position estimation, while the optimized covariance provides parameters for the LMB correlation probabilities, thereby enhancing the correlation between relative and absolute observations.

3) *LMB prediction and associated weight update*: Initially, we set a probability threshold, P_G . This threshold is based on the camera's detection range. Its purpose is to filter out newly born vehicles. We define these newcomers as part of the networking group. Simultaneously, it helps eliminate redundant Bernoulli information.

$$P_{non}(P(b_t^m = 0)) > P_G, \quad m \in \{0, 1, \dots, M_k\} \quad (17)$$

where P_{non} indicates the probability that the observation corresponding to the current particle state is not associated with the motion platform. Equation (17) indicates that the measurements correspond to particle states generated by newly born network members, rather than by surviving network members.

The state of the LMB-RFS motion platform is then combined with robot observations to generate particles using a likelihood function. This results in the generation of related parameters, including the particle state, particle weight, and multi-vehicle platform networking probability.

$$\omega_p^\ell = \frac{1}{N_p}, \quad x^\ell = K(o), \quad \ell \in L_k^*, \quad r^\ell = \frac{\mu_B}{M} p_{non}^\ell \quad (18)$$

where N_p is the total number of particles, x^ℓ is the spatial probability density function (pdf) of the particle. The function $K(\cdot)$ represents the likelihood function, and ω_p^ℓ is the initial weight of the particle. Additionally, r^ℓ is the existence probability of the robot, and μ_B is the probability of birth networking platform mean.

It is noted that the label space of new objects (\mathbb{B}) and the label space of existing objects (\mathbb{L}) are complementary and satisfy $\mathbb{B} \cap \mathbb{L} = \phi$. The RFS is then divided into two parts: the multi-Bernoulli RFS of the survived networked robots (marked as S) and the multi-Bernoulli RFS of the new birth network robots (marked as B).

$$X_{t+1}^* = X_t^{S*} \cup X_{t+1}^{B*} \quad (19)$$

where the superscript S indicates the members who have formed a surviving networked group at time t and in the networked group at the next time $t+1$ and its Bernoulli component is $\{(r_{S,t}^\ell, s_{S,t}^\ell(x_t))\}_{\ell \in L_t^{S*}}$. The superscript B means not in the networking group at step t , and a new member in the networking group at the next step $t+1$, that is, a new member and is the Bernoulli component. Those surviving members retain the Bernoulli information, and their corresponding label set fields follow as

$$\begin{cases} \mathbb{L}_{t+1}^{S*} = \mathbb{L}_t^{S*} \cup \mathbb{L}_{t+1}^{B*} \\ \mathbb{L}_t^{S*} \cap \mathbb{L}_{t+1}^{B*} = \phi \end{cases} \quad (20)$$

According to equation (15), the pdf of LMB-RFS can be expressed as

$$f(X^*) = \Delta(X^*) \prod_{\ell' \in \mathbb{L}^* \setminus \mathcal{L}(X^*)} (1 - r^{\ell'}) \prod_{x \in X^*} 1_{\mathbb{L}^*}(\ell) r^\ell s^\ell(x^n) \quad (21)$$

$$\mathcal{L}(X^*) \triangleq \{\ell^{(1)}, \ell^{(2)}, \dots, \ell^{(n)}\} \quad (22)$$

$$\Delta(X^*) = \delta_{|X^*|}(|\mathcal{L}(X^*)|) \quad (23)$$

where ℓ' is labelled as not participating in the networking, $\mathbb{1}_{\mathbb{L}^*}(\ell)$ is an inclusive function, and $\ell \in \mathbb{L}^*$ is 1, otherwise it is 0. $\mathcal{L}(X^*)$ represents the robot label set of LMB-RFS, δ is the Kronecker function.

Since the cardinality distribution of labelled RFS is the same as that of unlabeled RFS, the subscripts of $\delta_{|X^*|}$ is denoted the same label $X^* = (|\mathcal{L}(X^*)|)$, when the labels in X^* are independent of each other, $\Delta X^* = 1$ and 0 otherwise. The update of particle filtering on the new robotics platform.

$$f(X_{t+1}^* | o_t^*) = f(X_t^* | o_t^*, W_t^*) \quad (24)$$

where W_t^* is the noise set of networked robots, and then we update the existence probability, association weight by the parameter set $\pi = \{r^\ell, s^\ell\}_{\ell \in L}$, $(\ell, m) \in L^* \times \{1, \dots, M_t\}$.

$$\hat{r}_{t+1}^\ell = r_{t+1}^\ell \times P_S \quad (25)$$

$$\hat{\omega}_p^\ell = \omega_p^\ell \times \frac{1}{\sqrt{2\pi v_d v_\theta}} e^{-\frac{1}{2} \times \frac{\|\mathbf{o}_{ij}(1) - \mathbf{a}_{ij}^\ell\|^2}{v_d^2}} \times e^{-\frac{1}{2} \times \frac{\|\mathbf{o}_{ij}(2) - \theta_{ij}^\ell\|^2}{v_\theta^2}} \quad (26)$$

$$\beta_{t+1}^{\ell, m} = r_{t+1}^{\ell, m} \times \eta^{\ell, m} = r_{t+1}^\ell \times P_D \times \sum_{j=1}^{N_p} \hat{\omega}_p^\ell / \omega_{cul} \quad (27)$$

where P_S represents the survival probability of each robot at the specific moment. The variables $\mathbf{o}_{ij}(1)$ and $\mathbf{o}_{ij}(2)$ denote the distance and orientation information in the observation of the robot, respectively. Moreover, d_{ij}^ℓ and θ_{ij}^ℓ represent the relative distance and relative orientation of the neighbors, while v_d^2 and v_θ^2 are the variances of ranging noise and orientation, respectively. $\beta_{t+1}^{\ell, m}$ indicates association weights, P_D indicates the detection probability, ω_{cul} indicates the probability of incorrect observation, and N_p represents the number of particles of the filter.

4) *Probabilistic data association observation update based on belief propagation*: The edge association probability is determined by employing the belief propagation algorithm, which relies on the factor graph model. Once the association weights are updated, redundant variables are integrated into the model. For the association probability fast marginalization introduce the association vector \mathbf{a}_t and the corresponding variable \mathbf{b}_t [51].

$$\mathbf{a}_t^{(\ell)} \in \{-1, 0, \dots, M_t\}, \ell \in L_t^*, m \in \{-1, 0, 1, \dots, M_t\} \quad (28)$$

where $\mathbf{a}_t^{(\ell)} = m$ denotes the association variables corresponding to the ℓ -th robot state estimation and the m -th measurement. $m = 0$ indicates that it is not associated with any measurement, $m = -1$ indicates that it does not exist. When $\mathbf{b}_t^{(m)} = \ell \in \mathbb{L}_t^*$, it means that there is an observation related to the robot m . When $\mathbf{b}_t^{(m)} = 0$, it means that there is no observation related to the robot.

The joint associated probability mass function is

$$p(\mathbf{a}_t, \mathbf{b}_t) \propto \Psi(\mathbf{a}_t, \mathbf{b}_t) \prod_{\ell \in L_t^*} \hat{\beta}_t^{\ell, \mathbf{a}_t^{(\ell)}} \quad (29)$$

$$\Psi(\mathbf{a}_t, \mathbf{b}_t) = \prod_{\ell \in L_t^*} \prod_{m=1}^{M_t} \Psi_{\ell, m}(\mathbf{a}_t^{(\ell)}, \mathbf{b}_t^{(m)})$$

when $\mathbf{a}_t^{(\ell)} = m, \mathbf{b}_t^{(m)} \neq \ell$ or $\mathbf{a}_t^{(\ell)} \neq m, \mathbf{b}_t^{(m)} = \ell, \Psi(\mathbf{a}_t^{(\ell)}, \mathbf{b}_t^{(m)}) = 0$, and 1 otherwise, which defines the representation motion platform to match with the observation set. The message passing in the LMB collaborative navigation system, with the introduction of redundant variables, can be described as

$$\zeta_t^{[i] \ell \rightarrow m} = \frac{\hat{\beta}_t^{\ell, m}}{\hat{\beta}_t^{\ell, -1} + \hat{\beta}_t^{\ell, 0} + \sum_{\substack{m'=1 \\ m' \neq m}}^{M_k} \hat{\beta}_t^{\ell, m'} V_t^{[i-1] m' \rightarrow \ell}} \quad (30)$$

$$V_t^{[i] m \rightarrow \ell} = \frac{1}{1 + \sum_{\ell' \in L_t^*} \zeta_t^{[i-1] \ell' \rightarrow m}} \quad (31)$$

In equations (30) and (31), the inter-iterations are performed for each value of i until i takes on all values from 1 to I .

$$\hat{\beta}_t^{\ell, -1} = 1 - \hat{r}_t^\ell \quad (32)$$

$$\hat{\beta}_t^{\ell, 0} = \hat{r}_t^\ell \times (1 - P_D) \quad (33)$$

$$P_{ass}^\ell = P(\mathbf{a}_t^{(\ell)} = m) = \begin{cases} \hat{\beta}_t^{\ell, m} / D_t^\ell, m \in \{-1, 0\} \\ \hat{\beta}_t^{\ell, m} V_t^{m \rightarrow \ell} / D_t^\ell, m \in \{1, \dots, M_k\} \end{cases} \quad (34)$$

$$D_t^\ell = \hat{\beta}_t^{\ell, -1} + \hat{\beta}_t^{\ell, 0} + \sum_{m'=1}^{M_t} \hat{\beta}_t^{\ell, m'} V_t^{[I] m' \rightarrow \ell} \quad (35)$$

$$P_{non}^\ell = P(\mathbf{b}_t^m = 0) = \frac{1}{1 + \sum_{\ell' \in L_t^*} \zeta_t^{[I] \ell \rightarrow m}} \quad (36)$$

where P_{ass}^ℓ is the probability of correlation among robots, and P_{non}^ℓ is the probability that the observed value corresponding to the particle state is robot-independent, which is fed redundant Bernoulli information into the next iteration.

5) *Observations update*: The association weights are updated via messaging and the observations are modified accordingly. This includes the updated network probabilities and spatial probability density functions for grouped robots.

$$\hat{\omega}_{\mathbf{a}_t}^{(\ell)j} = \sum_{\substack{\ell \in L_t^* \\ m=0}}^{M_t} \hat{\beta}_t^{\ell, m} \times \hat{\omega}_{\mathbf{a}_t}^{(\ell)j}, m \in \{0, 1, \dots, M_t\} \quad (37)$$

$$\hat{\omega}_p^{(\ell)} = \frac{\hat{\omega}_{\mathbf{a}_t}^{(\ell)j}}{\sum_j^{N_p} \hat{\omega}_{\mathbf{a}_t}^{(\ell)j}} \quad (38)$$

$$\hat{r}_t^\ell = \sum \hat{\beta}_t^{\ell, m}, m \in \{0, 1, \dots, M_t\} \quad (39)$$

where $\hat{\omega}_{\mathbf{a}_t}^{(\ell)j}$ is the weight related to the observation and the robot, $\hat{\omega}_p^{(\ell)}$ is the updated particle weight, and j is the particle. \hat{r}_t^ℓ denotes the existence probability or networking probability.

Lastly, through standardized post-processing, pruning and resampling techniques for state estimation, we attain reliable robot presence probabilities \hat{r}_{t+1}^ℓ and state estimates $\hat{\mathbf{s}}_{t+1}^\ell$.

C. Optimization of communication structure

In this section, we adopt a multi-robot communication approach using a cyclic structure. The cyclic structure enables bidirectional information flow among robots, promoting a comprehensive exchange of observation and measurement data among neighbors [52].

In the state update process within the communication module, we design a novel approach to assign the coefficients in the state update equation based on the robot survival probability \hat{r}_t^ℓ obtained from the LMB filter. The state update equation is as

$$(\Sigma_{t+1}^i)^{-1} = c_0(\Sigma_t^i)^{-1} + \sum_{j \in C_{i,t}} c_j(\Sigma_t^j)^{-1} \quad (40)$$

$$\hat{s}_{t+1}^i = \Sigma_{t+1}^i \times \left[c_0(\Sigma_t^i)^{-1} \hat{s}_t^i + \sum_{j \in C_{i,t}} c_j(\Sigma_t^j)^{-1} \hat{s}_t^j \right] \quad (41)$$

where, c_0 and c_j represent the coefficients used to weight the fused robot states. By incorporating robot presence probabilities into the coefficient assignments, we can fuse the information from different neighboring robots.

V. LMB-GS-EPF ALGORITHM AND CONVERGENCE CONSISTENCY

A. LMB-GS-EPF algorithm

Our proposed algorithm aims to improve the accuracy and consistency of CL. The algorithm simultaneously estimates the robot's state and covariance by using parallel multimodal robot state update strategies such as motion model, observation model and communication model, as detailed in Algorithm 1. By the particle based LMB filtering algorithm, we couple relative and absolute observations. Moreover, we optimize the communication structure by means of a cyclic directed graph. Leveraging the robot existence probabilities computed by the LMB filter, we achieve an optimized allocation of coefficients in the state update equation. The LMB-GS-EPF algorithm we proposed can be summarized as follows:

- 1) Global State Representation: our LMB-GS-EPF employs a global state representation to capture the interrelationships and collaborative historical behaviors among multiple robots for enhancing localization accuracy.
- 2) Labeled Multi-Bernoulli Filter: our LMB-GS-EPF introduces the labeled multi-Bernoulli filter for modeling and labeling multi-robot state information as labeled RFS. It couples the relative and absolute observations, discarding negligibly weighted assumption and redundant computation. It retains the historical information with high confidence and offers a flexible state update strategy in communication mode, addressing the limitations in intermittent observation environments. The dynamic grouping process improves the computational efficiency and handles the scenarios with low detection probability and high false alarms without sacrificing the estimation accuracy.
- 3) Parallel Communication and Observation: our LMB-GS-EPF incorporates the parallelism by treating communication and observation as an integral mechanism. Using

a cyclic communication topology, the algorithm assigns the coefficients based on the existence probability of the Bernoulli filter. This approach enhances flexibility and scalability, resulting in more robust and efficient multi-robot systems.

Algorithm 1 LMB-GS-EPF by Robot i

Initialization

Set \hat{S}_0^i and Σ_0^i for robot i .

Motion Model

input: odometer v_t^i

$$\hat{S}_{t+1}^i = [f_1^T(\hat{s}_{1,t}^i, v_t^i), \dots, f_i^T(\hat{s}_{i,t}^i, v_t^i), \dots, f_M^T(\hat{s}_{M,t}^i, v_t^i)]^T,$$

$$\Sigma_{t+1}^i = \Sigma_t^i + \Sigma^{qi} = \Sigma_t^i + \text{Diag}(\Sigma^{u1}, \dots, \Sigma^{uM}).$$

Observation Model

input: camera o^{ij}

$$\hat{S}_{t+1}^i = \hat{S}_{1,t}^i + \Sigma_t^i H^{ijT} R_{o^{ij}}^{-1} (o^{ij} - H^{ij} \hat{S}_t^i),$$

$$(\Sigma_{t+1}^i)^{-1} = (\Sigma_t^i)^{-1} + (H^i)^T C(\theta_t^i) R_{o^{ij}}^{-1} C^T(\theta_t^i) H^i,$$

Determine the particle and weight $\{s_{0:t+1}^i, \omega_{t+1}^i\}_{j=1}^{N_p}$,

Optimization of robot state \hat{s}_{t+1}^i using PF algorithm.

LMB Initial

Determine \mathbb{L}_B^* using $P_{non}^\ell > P_G$, according to $P_{non}^\ell = P(b_t^m = 0)$ given P_G , $m \in \{0, 1, \dots, M_k\}$, create new Bernoulli component $\{r^i, s^i\}_{i=1}^M$.

LMB propagation

Determine \hat{r}_{t+1}^ℓ and $\hat{\omega}_p^\ell$.

Associated weight update

Determine $\beta_{t+1}^{(\ell,m)}$, $m \in \{-1, 0, 1, \dots, M_t\}$, with $\beta_{t+1}^{(\ell,m)}$, $m = -1$, with $\beta_{t+1}^{(\ell,m)}$, $m = 0$, with $\beta_{t+1}^{(\ell,m)}$, $m \in \{1, \dots, M_t\}$,

Determine $\hat{\omega}_{a_{t+1}}^{(\ell)j}$.

LMB-BP Message Passing I interactions

Determine $\zeta_{t+1}^{[i] \ell \rightarrow m} \rightleftharpoons V_{t+1}^{[i-1] \ell \rightarrow m}$, i is the interaction index,

Determine $P_{ass}^\ell = P(a_{t+1}^\ell = m)$ and $P_{non}^\ell = P(b_{t+1}^m = 0)$.

Probabilities update and spatial probability update

Calculation of $\hat{\omega}_p^{(\ell)}$ and \hat{r}_{t+1}^ℓ using equations (38) and (39), Post-processing by pruning and re-sampling to optimize \hat{s}_{t+1}^i and Σ_{t+1}^i .

Communication Model

input: \hat{s}_t^k, Σ_t^k from robot k

$$(\Sigma_{t+1}^i)^{-1} = c_0(\Sigma_t^i)^{-1} + \sum_{j \in C_{i,t}} c_j(\Sigma_t^j)^{-1},$$

$$\hat{s}_{t+1}^i = \Sigma_{t+1}^i \times \left[c_0(\Sigma_t^i)^{-1} \hat{s}_t^i + \sum_{j \in C_{i,t}} c_j(\Sigma_t^j)^{-1} \hat{s}_t^j \right],$$

The allocation of coefficients to c_0 and c_j is determined based on the presence probability of the robot transmitting the message.

B. Convergence consistency proof

First, we establish the convergence consistency of the message-passing algorithm. Subsequently, we demonstrate the convergence consistency of the message-passing embedded within the explicit communication algorithm.

We establish the fractional forms of equations (30) and (31) in accordance with the requirements of the guaranteed

convergence proof. By using the fractional expression function f in equation (30), we construct the representation distance function d such that there exists a contraction factor $\alpha < 1$ satisfying $d(f(x), f(y)) \leq \alpha d(x, y), \forall (x, y)$ [54]. When the function f is in fractional form, any sequence derived from repeated applications of the function f converges to the same fixed value. Subsequently, the measure for information is defined as

$$d(\zeta, V) = \max\left\{\max_{\ell, m} \frac{\zeta^{\ell \rightarrow m}}{V^{m \rightarrow \ell}}, \max_{\ell, m} \frac{V^{\ell \rightarrow m}}{\zeta^{m \rightarrow \ell}}\right\} \quad (42)$$

The dynamic log distance form is defined as

$$d(f(x), f(y)) \leq d(x, y)^\alpha, \forall (x, y) \quad (43)$$

so that $\log d(f(x), f(y)) \leq \alpha \log d(x, y), \forall (x, y)$.

We define the update $\zeta^{\ell \rightarrow m} = f(V^{m \rightarrow \ell})$ in equation (30), and $\zeta^{m \rightarrow \ell} = g(V^{\ell \rightarrow m})$ in equation (31). Now, we present a list of preliminary lemmas concerning the form of the contraction factor that will be utilized.

Lemma 1 [53]. For $c > 0$ and $L > 1$, we have the following

$$\alpha(L, c) = \frac{\log\left(\frac{1+cL}{1+c}\right)}{\log L} \quad (44)$$

The function value is strictly less than 1 and increases monotonically with L .

The following two lemmas demonstrate that the LMB-RFS updates in equations (30) and (31) are contractions.

Lemma 2. For all (V, \tilde{V}) with $d(V, \tilde{V}) \leq \bar{L}$, The update of message $f(\cdot)$ in equation (30) is a contraction about the dynamic distance measure $d(\cdot, \cdot)$ with the factor $\alpha(\bar{L}, m_t W)$, i.e.,

$$d(f(V), f(\tilde{V})) \leq d(V, \tilde{V})^{\alpha(\bar{L}, m_t W)} \quad (45)$$

where $m_t W = \max_{\ell, m} \frac{\sum_{m' \neq m}^{M_k} \hat{\beta}_{t+1}^{(\ell, m')}}{\hat{\beta}_{t+1}^{(\ell, -1)} + \hat{\beta}_{t+1}^{(\ell, 0)}}$.

Proof. It is assumed that $\forall (\ell, m)$, $\zeta^{\ell, m}$ and $\tilde{\zeta}^{\ell, m}$ bounded with $0 < \zeta^{\ell, m} \leq 1$ and $0 < \tilde{\zeta}^{\ell, m} \leq 1$, when $\zeta^{\ell, m}$ or $\tilde{\zeta}^{\ell, m}$ is zero, it guarantees any $(\zeta, \tilde{\zeta})$ resulting from equation (31), let

$$1 \leq L \triangleq d(V, \tilde{V}) \leq \bar{L} < \infty \quad (46)$$

It is easy that $V^{\ell, m} \leq L \tilde{V}^{\ell, m}$ and $\tilde{V}^{\ell, m} \leq L V^{\ell, m}$.

Since the association weight $\hat{\beta}^{(\ell, m)}$ is non-negative and bounded, if $\hat{\beta}^{(\ell, m)} = 0$ then in equation (30), $i = I$ and the superscript of iteration process I is omitted, get $f(V^{\ell, m}) = f(\tilde{V}^{\ell, m}) = 0$ and $f(V^{\ell, m})/f(\tilde{V}^{\ell, m}) = 0/0 \triangleq 1$. Otherwise, the division is considered.

Define $\hat{\beta}_{t+1}^{(\ell, -1)} + \hat{\beta}_{t+1}^{(\ell, 0)} \triangleq A$, one obtains the following.

$$\begin{aligned} \frac{f(V^{\ell, m})}{f(\tilde{V}^{\ell, m})} &= \frac{\hat{\beta}_{t+1}^{(\ell, -1)} + \hat{\beta}_{t+1}^{(\ell, 0)} + \sum_{m' \neq m}^{M_k} \hat{\beta}_{t+1}^{(\ell, m')} \tilde{V}_{t+1}^{m' \rightarrow \ell}}{\hat{\beta}_{t+1}^{(\ell, -1)} + \hat{\beta}_{t+1}^{(\ell, 0)} + \sum_{m' \neq m}^{M_k} \hat{\beta}_{t+1}^{(\ell, m')} V_{t+1}^{m' \rightarrow \ell}} \\ &= \frac{A + \sum_{m' \neq m}^{M_k} \hat{\beta}_{t+1}^{(\ell, m')} \tilde{V}_{t+1}^{m' \rightarrow \ell}}{A + \sum_{m' \neq m}^{M_k} \hat{\beta}_{t+1}^{(\ell, m')} V_{t+1}^{m' \rightarrow \ell}} \\ &\leq \frac{A + \sum_{m' \neq m}^{M_k} \hat{\beta}_{t+1}^{(\ell, m')} L V_{t+1}^{m' \rightarrow \ell}}{A + \sum_{m' \neq m}^{M_k} \hat{\beta}_{t+1}^{(\ell, m')} V_{t+1}^{m' \rightarrow \ell}} \end{aligned} \quad (47)$$

Define $c = (\sum_{m' \neq m}^{M_k} \hat{\beta}_{t+1}^{(\ell, m')} V_{t+1}^{m' \rightarrow \ell}) / (\hat{\beta}_{t+1}^{(\ell, -1)} + \hat{\beta}_{t+1}^{(\ell, 0)})$

$$\frac{f(V^{\ell, m})}{f(\tilde{V}^{\ell, m})} = \frac{A + cAL}{A + cA} = \frac{1 + cL}{1 + c} \quad (48)$$

where $c = \frac{\sum_{m' \neq m}^{M_k} \hat{\beta}_{t+1}^{(\ell, m')} V_{t+1}^{m' \rightarrow \ell}}{\hat{\beta}_{t+1}^{(\ell, -1)} + \hat{\beta}_{t+1}^{(\ell, 0)}} \leq m_t W$.

Using Lemma 1

$$\begin{aligned} \frac{f(V^{\ell, m})}{f(\tilde{V}^{\ell, m})} &= \frac{1 + cL}{1 + c} \\ &\leq \frac{1 + m_t WL}{1 + m_t W} = L^{\alpha(L, m_t W)} \leq L^{\alpha(\bar{L}, m_t W)} \end{aligned} \quad (49)$$

Those similar steps are followed as

$$\frac{f(\tilde{V}^{\ell, m})}{f(V^{\ell, m})} \leq \frac{1 + m_t WL}{1 + m_t W} \leq L^{\alpha(\bar{L}, m_t W)} \quad (50)$$

Now we establish the same validation of interactive step in equation (31).

Lemma 3. For all $(\zeta, \tilde{\zeta})$ with $d(\zeta, \tilde{\zeta}) \leq \bar{L}$, The update of message $g(\cdot)$ in equation (30) is a contraction about the dynamic distance measure with $d(\cdot, \cdot)$ the factor $\alpha(\bar{L}, \ell_t W)$, i.e.,

$$d(g(\zeta), g(\tilde{\zeta})) \leq d(\zeta, \tilde{\zeta})^{\alpha(\bar{L}, \ell_t W)} \quad (51)$$

Proof It is assumed that $\forall (\ell, m)$, $V^{\ell, m}$ and $\tilde{V}^{\ell, m}$ bounded with $0 \leq V^{\ell, m} \leq 1$, if $V^{\ell, m}$ or $\tilde{V}^{\ell, m}$ is 0, it guarantees any $d(\zeta, \tilde{\zeta})$ resulting from equation (31), let

$$1 \leq L \triangleq d(\zeta, \tilde{\zeta}) \leq \bar{L} < \infty \quad (52)$$

We prove it in the same step,

$$\begin{aligned} \frac{g(\zeta^{\ell, m})}{g(\tilde{\zeta}^{\ell, m})} &= \frac{1 + \sum_{\ell' \in \mathcal{L}_{t+1}^*} \tilde{\zeta}_{t+1}^{\ell' \rightarrow m}}{1 + \sum_{\ell' \in \mathcal{L}_{t+1}^*} \zeta_{t+1}^{\ell' \rightarrow m}} \leq \frac{1 + \ell_t WL}{1 + \ell_t W} \leq L^{\alpha(\bar{L}, \ell_t W)} \\ \frac{g(\tilde{\zeta}^{\ell, m})}{g(\zeta^{\ell, m})} &\leq \frac{1 + \ell_t WL}{1 + \ell_t W} \leq L^{\alpha(\bar{L}, \ell_t W)} \end{aligned} \quad (53)$$

Now we present Theorem 1 to prove LMB-GS-EPF algorithm's convergence consistency when the robot information source is camera to landmark absolute observation data or camera to neighborhood robot relative observation data.

Theorem 1. Regardless of different initializations, GS-EPF-LMB iterative operations $f(\cdot)$ in equation (30), $g(\cdot)$ in equation (31) will converge to the same point.

Proof Let us start with an initial vector $V_0^{[1]m \rightarrow \ell}$. Then, using equation (30), we have $\zeta_0^{[2]m \rightarrow \ell} = f(V_0^{[1]m \rightarrow \ell})$. Now, consider the iteration process $\zeta_0^{[i]m \rightarrow \ell} = f(g(\zeta_0^{[i-1]m \rightarrow \ell}))$. We can see that $L = d(\zeta_0, \zeta_1) < \infty$, where d is the distance function measuring the difference between ζ_0 and ζ_1 .

Using Lemmas 2 and 3 $d(\zeta_k, \zeta_{k+1}) \leq L^{\alpha(\bar{L}, \max\{m_t, n_t\} W)} 2^{Ik}$. When $L^{\alpha(\bar{L}, \max\{m_t, n_t\} W)} \rightarrow 1$.

When the robot has no available information source, the GS-EPF-LMB algorithm uses a new communication mechanism to update the estimates and its convergence consistency follows [29].

TABLE I
SYMBOL OR VARIABLE DESCRIPTIONS

Symbol	Description
\mathbb{S}_t	State set of multiple robots
v_t^i	Linear velocity of robot i at time t
ω_t^i	Angular velocity of robot i at time t
θ_t^i	Heading of robot i at time t
o^{ij}	Observation of robot i on target j (neighbor robot or landmark)
C	Rotation matrix related to heading
H	Linear innovation matrix in the observation model
Σ_t^i	State covariance of robot i at time t
$R_{o^{ij}}$	Covariance matrix of measurement noise
X_t	State set of multiple robots at time t with associated labels
o_t^*	Observation set at time t
$\pi(X)$	Prior probability distribution function of an LMB-RFS
X_t^*	LMB-RFS component information set of multiple robots
r_t^ℓ	Probability of the existence of a labeled robot
$s_t^\ell(x_t^i)$	State information of robot i with label ℓ
P_G	Given probability threshold for camera-based detection range to filter out newly born vehicles
P_{non}	Probability that the current particle state corresponds to an observation independent of the motion platform
ω_p^ℓ	Particle weight corresponding to robot label ℓ
$K(o)$	Likelihood function related to observation
$\beta_{t+1}^{(\ell,m)}$	At time $t+1$, the robot-associated weights labeled as ℓ
α_1, α_2	Coefficients for weighted fusion of robot states in communication update mode

The table focuses on the key symbols and variables involved in the algorithm of this paper.

C. Symbol Description

This section lists important symbols and variable descriptions in the article, as shown in Table I.

VI. EXPERIMENT

This section presents the experimental dataset, outlines baseline methodologies for comparison, specifies evaluation metrics, and explains experiment results.

A. Experimental Dataset

The proposed LMB-GS-EPF algorithm's performance was evaluated using the UTIAS multi-robot CL and mapping dataset provided by Leung et al [55]. Each robot was equipped with a wheel encoder and a monocular camera, measuring linear and rotational velocities at 67 Hz and capturing distance and orientation measurements with other robots and landmarks. The position and orientation were obtained from a 10-camera Vicon motion capture system at 100 Hz, with a positional accuracy of approximately 1 mm.

B. Compared Baselines

We compared the proposed approach with two representative SOTA algorithms, including EKF-based DCL [29], [56] and EKF-based CCL [12], [57].

C. Evaluation Metrics

The paper evaluated the algorithm using two commonly indicators for CL: positioning error (RMSE) and state covariance estimation error, corresponding to equations (54) and (55) respectively.

$$\sqrt{\sum_{i=1}^N \|\hat{s}_t^i - s_t^i\|^2 / N} \quad (54)$$

$$\sqrt{\sum_{i=1}^N \text{tr}([\Sigma_{s^i}]_i) / N} \quad (55)$$

D. Results

We executed all the algorithms and gathered the performance data in two key dimensions: the accuracy of robot localization and the precision of tracking covariance estimation. Additionally, we recorded the computational time each algorithm consumed when applied to a 3-robot dataset operating on a 200-second cycle. The comprehensive evaluation outcomes have been organized and are showcased in Table II. The metrics encompassed within the table include localization error (measured in meters), tracking covariance (expressed in square meters), and time cost (quantified in seconds). To ensure a comprehensive assessment, we compared our algorithm (Our) with the DCL-based GS-CI algorithm and the CCL-based Cen-EKF algorithm. The tested localization accuracy results were presented in Fig. 1. In this figure, the localization accuracies of each robot associated with the various methods were shown in the same subplot, with the vertical coordinate indicating the localization accuracy and the horizontal coordinate indicating the time series.

To enhance clarity, we had divided the axis into four segments spanning from 0 to 200. Notably, our algorithm consistently demonstrates exceptional performance in localization accuracy and maintain an accuracy of approximately 0.1 meters. This result stands as a testament to the robustness of the algorithm we developed. To validate the algorithm's consistency, we undertook a comparable evaluation of tracking covariance accuracy. The outcomes are presented in Fig. 2. Our algorithm significantly advances the tracking covariance accuracy in comparison to the GS-CI algorithm. This achievement can be attributed to the innovative cyclic communication topology we formulated, and the strategic assignment of communication update coefficients based on existence probabilities.

TABLE II
ALGORITHM PERFORMANCE COMPARISON

Method		Loc_error (m)	Trace_Cov (m ²)	Time Cost (s)
DCL	GS-SCI [56]	0.142	1.871	13.578
	GS-CI [29]	0.135	1.254	12.717
	Our	0.095	0.536	14.651
CCL	EKF-LS-CI [12]	0.492	0.120	10.683
	Cen-EKF [57]	0.138	0.115	10.759

Evaluation results of all algorithms on the 3-robot dataset with a period of 200 seconds for the system as a whole.

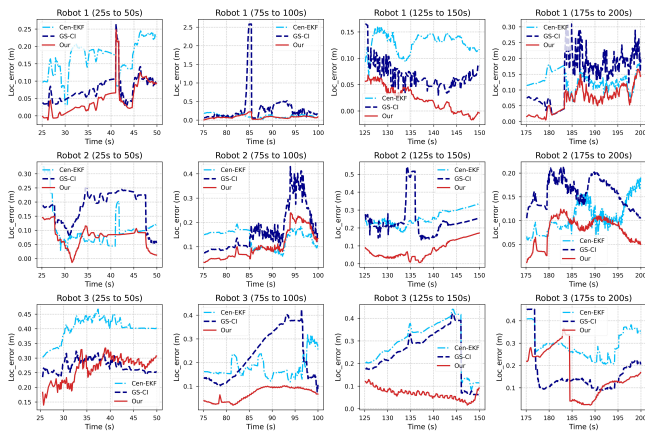


Fig. 1. Comparison of localization accuracy of all the algorithms corresponding to the three robots.

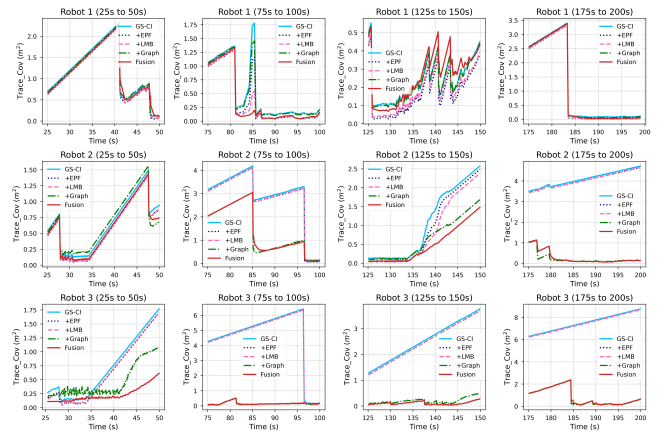


Fig. 4. Tracking covariance accuracy results of ablation experiments.

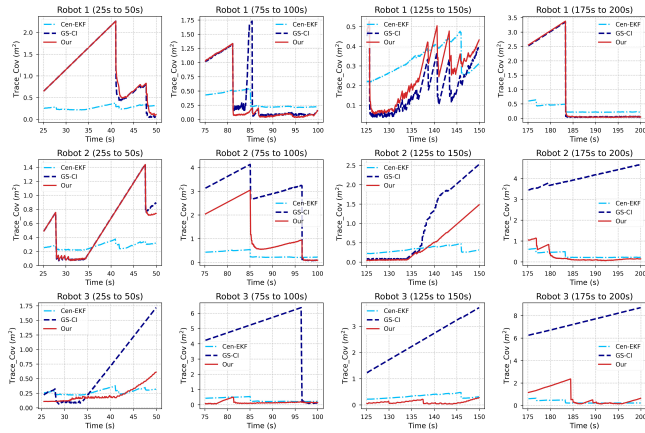


Fig. 2. Comparison of tracking covariance accuracy for all the algorithms corresponding to the three robots.

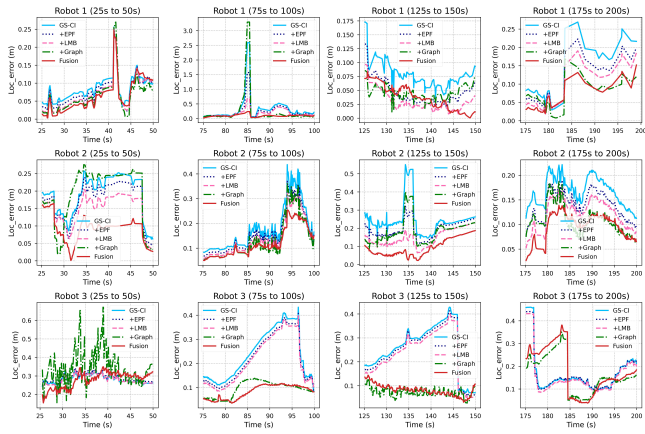


Fig. 3. Localization accuracy results of ablation experiments.

E. Ablation Experiment

A series of ablation experiments was conducted. This involved the stepwise integration of individual improvements,

EPF, LMB filtering, and communication structure Graph optimization into the GS-CI algorithm [29]. The experimental results are shown in Fig. 3 and Fig. 4, where the Fusion curve represents the integration of all three improvements in the proposed LMB-GS-EPF algorithm.

Firstly, in our experimental setup where we introduced the EPF, we witnessed a discernible reduction in the localization error when contrasted with the GS-CI algorithm.

After the integration of LMB filtering, we observed a stabilization in localization accuracy, settling around 0.11 meters, as demonstrated by the +LMB curve in Fig. 3. This result is attributed to the fact that the LMB algorithm we designed incorporates both relative and absolute observations.

In addition, we adopted a cyclic-structured directed graph for multi-robot communication to realize the bidirectional information flow between robots, while the coefficient assignments in the updating equations (40) are accomplished with the help of the robot survival probabilities obtained in the LMB filter while considering more historical information. As shown in the +Graph curve in Fig. 4, the tracking covariance accuracy of the robots is significantly improved, ensuring robust state consistency.

VII. CONCLUSION AND FUTURE WORK

This paper introduced a novel distributed cooperative localization algorithm (LMB-GS-EPF) tailored for multi-robot systems. This algorithm seamlessly integrates the motion, observation, and communication strategies, ensuring the concurrent state and covariance estimation robustness and consistency. By investigating the fusion of absolute and relative observations using the LMB filter and considering the incorporation of more reliable historical observations, the algorithm's impact on Cooperative Localization was analyzed. Additionally, the optimization of multi-robot communication topology and the refinement of communication updates, guided by the robot presence probability within the LMB filter, were achieved. The robustness and convergence of the proposed algorithm was validated through theory and quantitative results. The following conclusions are derived:

- 1) The integration of PF into the EKF-based CL algorithm effectively mitigated the linear truncation issue. Experimental results demonstrated the complementary nature of PF and EKF, leading to improved accuracy and consistency in CL. These improvements are particularly valuable when dealing with the models of LMB-RFS.
- 2) The modeling of inter-vehicle relative observations and landmark absolute observations as RFSs, coupled with the LMB filter, showcased a remarkable enhancement in positioning accuracy.
- 3) The proposed cyclic communication topology, coupled with the inter-iterations coefficient allocation based on robot survive probability and existence probability of the LMB filter, significantly improved the tracking covariance accuracy by 50%.

Our work suggests several avenues for potential improvements in the field of CL. One promising avenue involves exploring the integration of diverse sensors, such as visual sensors, lidar, and radar, to bolster adaptability and accuracy across various environmental conditions. Furthermore, enhancing communication strategies and investigating dynamic reconfiguration techniques to accommodate evolving network conditions could significantly augment the algorithm's robustness. These future research directions hold great potential for advancing CL, enabling it to excel in real-world scenarios and broadening its applications.

REFERENCES

- [1] Hu, Junyan, et al. "Fault-tolerant cooperative navigation of networked UAV swarms for forest fire monitoring." *Aerospace Science and Technology* 123 (2022): 107494.
- [2] Wang, Yuanda, et al. "Cooperative USV-UAV marine search and rescue with visual navigation and reinforcement learning-based control." *ISA transactions* (2023).
- [3] de Alcantara Andrade, Fabio Augusto, et al. "Autonomous unmanned aerial vehicles in search and rescue missions using real-time cooperative model predictive control." *Sensors* 19.19 (2019): 4067.
- [4] Wang, Z. H., et al. "An intelligent ground-air cooperative navigation framework based on visual-aided method in indoor environments, Unmanned Syst. 9 (3)(2021) 237–246."
- [5] Allotta, Benedetto, et al. "Cooperative navigation of AUVs via acoustic communication networking: field experience with the Typhoon vehicles." *Autonomous Robots* 40 (2016): 1229-1244.
- [6] Liu, Zhe, et al. "Visuomotor reinforcement learning for multirobot cooperative navigation." *IEEE Transactions on Automation Science and Engineering* 19.4 (2021): 3234-3245.
- [7] Gans, Nicholas R., and John G. Rogers. "Cooperative multirobot systems for military applications." *Current Robotics Reports* 2 (2021): 105-111.
- [8] Li, Zhi, et al. "Development status and key navigation technology analysis of autonomous underwater vehicles." 2020 3rd International Conference on Unmanned Systems (ICUS). IEEE, 2020.
- [9] Seco, Fernando, Antonio R. Jiménez, and Xufei Zheng. "RFID-based centralized cooperative localization in indoor environments." 2016 International Conference on Indoor Positioning and Indoor Navigation (IPIN). IEEE, 2016.
- [10] Chakraborty, Anusna, Rajnikant Sharma, and Kevin Brink. "Cooperative localization for multi-rotor UAVs." *AIAA Scitech* 2019 Forum. 2019.
- [11] Chakraborty, Anusna, et al. "Cooperative localization for fixed wing unmanned aerial vehicles." 2016 IEEE/ION Position, Location and Navigation Symposium (PLANS). IEEE, 2016.
- [12] Kia, Solmaz S., Stephen F. Rounds, and Sonia Martínez. "A centralized-equivalent decentralized implementation of extended Kalman filters for cooperative localization." 2014 IEEE/RSJ international conference on intelligent robots and systems. IEEE, 2014.
- [13] Kia, Solmaz S., Stephen Rounds, and Sonia Martínez. "Cooperative localization for mobile agents: A recursive decentralized algorithm based on Kalman-filter decoupling." *IEEE Control Systems Magazine* 36.2 (2016): 86-101.
- [14] Kia, Solmaz S., Stephen Rounds, and Sonia Martínez. "Cooperative localization under message dropouts via a partially decentralized EKF scheme." 2015 IEEE International Conference on Robotics and Automation (ICRA). IEEE, 2015.
- [15] Yin, Lu, Qiang Ni, and Zhongliang Deng. "Intelligent multisensor cooperative localization under cooperative redundancy validation." *IEEE transactions on cybernetics* 51.4 (2019): 2188-2200.
- [16] Burchett, Bradley. "A centralized extended Kalman filter for cooperative localization of munition swarms." *AIAA Aviation* 2019 Forum. 2019.
- [17] Su, Shaoshu, Pengxiang Zhu, and Wei Ren. "Multirobot Fully Distributed Active Joint Localization and Target Tracking." *IEEE Transactions on Control Systems Technology* (2023).
- [18] Huang, Yulong, et al. "Adaptive recursive decentralized cooperative localization for multirobot systems with time-varying measurement accuracy." *IEEE Transactions on Instrumentation and Measurement* 70 (2021): 1-25.
- [19] Carrillo-Arce, Luis C., et al. "Decentralized multi-robot cooperative localization using covariance intersection." 2013 IEEE/RSJ International Conference on Intelligent Robots and Systems. IEEE, 2013.
- [20] Yang, Qifan, et al. "Distributed cooperative localization based on bearing-only sensors." *IEEE Sensors Journal* 21.20 (2021): 23645-23657.
- [21] Chiella, Antonio CB, Bruno OS Teixeira, and Guilherme AS Pereira. "Robust attitude estimation using an adaptive unscented Kalman filter." 2019 International Conference on Robotics and Automation (ICRA). IEEE, 2019.
- [22] Wang, Dongjia, et al. "Resilient Decentralized Cooperative Localization for Multi-Source Multi-Robot System." *IEEE Transactions on Instrumentation and Measurement* (2023).
- [23] Leung, Keith YK, Timothy D. Barfoot, and Hugh HT Liu. "Decentralized localization for dynamic and sparse robot networks." 2009 IEEE International Conference on Robotics and Automation. IEEE, 2009.
- [24] Su, Huaicheng. "An Improved Approach For Multi-Robot Localization." (2008).
- [25] Bailey, Tim, et al. "Decentralised cooperative localisation for heterogeneous teams of mobile robots." 2011 IEEE International Conference on Robotics and Automation. IEEE, 2011.
- [26] Zhu, Jianan, and Solmaz S. Kia. "Cooperative localization under limited connectivity." *IEEE Transactions on Robotics* 35.6 (2019): 1523-1530.
- [27] Chang, Tsang-Kai, Kenny Chen, and Ankur Mehta. "Resilient and consistent multirobot cooperative localization with covariance intersection." *IEEE Transactions on Robotics* 38.1 (2021): 197-208.
- [28] Luft, Lukas, et al. "Recursive decentralized localization for multi-robot systems with asynchronous pairwise communication." *The International Journal of Robotics Research* 37.10 (2018): 1152-1167.
- [29] Chang, Tsang-Kai, Shengkang Chen, and Ankur Mehta. "Multirobot cooperative localization algorithm with explicit communication and its topology analysis." *Robotics Research: The 18th International Symposium ISRR*. Springer International Publishing, 2020.
- [30] Papaioannou, Savvas, et al. "Decentralized search and track with multiple autonomous agents." 2019 IEEE 58th Conference on Decision and Control (CDC). IEEE, 2019.
- [31] Dames, Philip M. "Distributed multi-target search and tracking using the PHD filter." *Autonomous robots* 44.3-4 (2020): 673-689.
- [32] Deusch, Hendrik, Stephan Reuter, and Klaus Dietmayer. "The labeled multi-Bernoulli SLAM filter." *IEEE Signal Processing Letters* 22.10 (2015): 1561-1565.
- [33] Gao, Lin, Giorgio Battistelli, and Luigi Chisci. "Random-finite-set-based distributed multirobot SLAM." *IEEE Transactions on Robotics* 36.6 (2020): 1758-1777.
- [34] Zhang, Feihu, et al. "Multiple vehicle cooperative localization under random finite set framework." 2013 IEEE/RSJ International Conference on Intelligent Robots and Systems. IEEE, 2013.
- [35] Wang, Bailu, et al. "Distributed fusion with multi-Bernoulli filter based on generalized covariance intersection." *IEEE Transactions on Signal Processing* 65.1 (2016): 242-255.
- [36] Papaioannou, Savvas, et al. "Probabilistic search and track with multiple mobile agents." 2019 International Conference on Unmanned Aircraft Systems (ICUAS). IEEE, 2019.
- [37] Zhang, Feihu, Christian Buckl, and Alois Knoll. "Multiple vehicle cooperative localization with spatial registration based on a probability hypothesis density filter." *Sensors* 14.1 (2014): 995-1009.
- [38] Hlinka, Ondrej, et al. "Distributed data fusion using iterative covariance intersection." 2014 IEEE International Conference on Acoustics, Speech and Signal Processing (ICASSP). IEEE, 2014.
- [39] Reuter, Stephan, et al. "The labeled multi-Bernoulli filter." *IEEE Transactions on Signal Processing* 62.12 (2014): 3246-3260.

- [40] Reuter, Stephan, et al. "A fast implementation of the labeled Bernoulli filter using Gibbs sampling." 2017 IEEE Intelligent Vehicles Symposium (IV). IEEE, 2017.
- [41] Li, Tiancheng, Juan M. Corchado, and Shudong Sun. "On generalized covariance intersection for distributed PHD filtering and a simple but better alternative." 2017 20th International Conference on Information Fusion (Fusion). IEEE, 2017.
- [42] Yi, Wei, et al. "Computationally efficient distributed multi-sensor fusion with multi-Bernoulli filter." IEEE Transactions on Signal Processing 68 (2019): 241-256.
- [43] Roumeliotis, Stergios I., and George A. Bekey. "Distributed multirobot localization." IEEE transactions on robotics and automation 18.5 (2002): 781-795.
- [44] Li, Suqi, et al. "Computationally efficient distributed multi-sensor multi-Bernoulli filter." 2018 21st International Conference on Information Fusion (FUSION). IEEE, 2018.
- [45] Vo, Ba-Ngu, Ba-Tuong Vo, and Michael Beard. "Multi-sensor multi-object tracking with the generalized labeled multi-Bernoulli filter." IEEE Transactions on Signal Processing 67.23 (2019): 5952-5967.
- [46] Gao, Lin, Giorgio Battistelli, and Luigi Chisci. "Fusion of labeled RFS densities with minimum information loss." IEEE Transactions on Signal Processing 68 (2020): 5855-5868.
- [47] Chen, Bo, et al. "Distributed covariance intersection fusion estimation for cyber-physical systems with communication constraints." IEEE Transactions on Automatic Control 61.12 (2016): 4020-4026.
- [48] Dames, Philip, and Vijay Kumar. "Cooperative multi-target localization with noisy sensors." 2013 IEEE International conference on robotics and automation. IEEE, 2013.
- [49] Bailey, Tim, et al. "Consistency of the EKF-SLAM algorithm." 2006 IEEE/RSJ International Conference on Intelligent Robots and Systems. IEEE, 2006.
- [50] Shariati, Hamid, Hassan Moosavi, and Mohammad Danesh. "Application of particle filter combined with extended Kalman filter in model identification of an autonomous underwater vehicle based on experimental data." Applied Ocean Research 82 (2019): 32-40.
- [51] Meyer, Florian, et al. "Message passing algorithms for scalable multi-target tracking." Proceedings of the IEEE 106.2 (2018): 221-259.
- [52] Wang, Shizhuang, et al. "Performance estimation for Kalman filter based multi-agent cooperative navigation by employing graph theory." Aerospace Science and Technology 112 (2021): 106628.
- [53] Williams, Jason L., and Roslyn A. Lau. "Convergence of loopy belief propagation for data association." 2010 Sixth International Conference on Intelligent Sensors, Sensor Networks and Information Processing. IEEE, 2010.
- [54] Koller, Daphne, and Nir Friedman. Probabilistic graphical models: principles and techniques. MIT press, 2009.
- [55] Leung, Keith YK, et al. "The UTIAS multi-robot cooperative localization and mapping dataset." The International Journal of Robotics Research 30.8 (2011): 969-974.
- [56] Li, Hao, and Fawzi Nashashibi. "Cooperative multi-vehicle localization using split covariance intersection filter." IEEE Intelligent transportation systems magazine 5.2 (2013): 33-44.
- [57] Mendes, Pedro, and Pedro Batista. "A study on cooperative navigation of AUVs based on bearing measurements." OCEANS 2021: San Diego-Porto. IEEE, 2021.



Hongmei Chen received the M.S. and Ph.D. degrees in Navigation Guidance and Control from Southeast University, China, in 2007 and 2015, respectively. Her research interests include GNSS positioning in challenging environments and localization for pedestrian, autonomous driving vehicle, and unmanned aerial vehicle. She is currently an associate professor in the Department of Electrical Engineering, Henan University of Technology. Her project focuses on highly interactive and adaptive vehicles

multivehicle cooperative localization, information processing and intelligent algorithm.



Haifeng Wang received the B.S. degree from Joint training of Ningxia Institute of Technology and Zhejiang University of Technology, Ningxia and Zhejiang, China, in 2021. He is currently pursuing the M.S. degree in electronic information at Henan University of Technology, Zhengzhou, China. His research interests include inertial navigation, INS/GPS integrated navigation, and visual-inertial navigation for autonomous vehicles.



Wen Ye (Member, IEEE) received the B.S. degree from Luoyang Institute of Science and Technology, Luoyang, China, in 2011, the M.S. degree from North China Electric and Power University, Beijing, China, in 2014, the Ph.D. degree from the Key Laboratory of Fundamental Science for National Defense-Novel Inertial Instrument and Navigation System Technology, Beijing University of Aeronautics and Astronautics, Beijing, China, 2018. His is currently with Institute of mechanics and acoustics metrology,

National Institute of Metrology, Beijing, China. His research interests include inertial navigation, INS/GPS integrated navigation, and visual-inertial navigation for autonomous vehicles and intelligent algorithm.



Dongbing Gu (Senior member, IEEE) received the B.S. degree from Beijing Institute of Technology, Beijing, China, in 1985, the M.S. degree from Beijing Institute of Technology, Beijing, China, in 1988, the Ph.D. degree from University of Essex, Colchester, UK, in 2004. He is currently a professor in the School of Computer Science and Electronic Engineering, University of Essex. His main research interests include robotics, autonomous systems, machine learning, multi-robot systems, cooperative control,

SLAM, UAVs, and process automation. He has significant research experience in developing advanced robotic technologies and his research has been funded by UK Research Councils (EPSRC), Innovate UK, Royal Society, European Commission, British Council as well as industrial companies. He has published more than 200 scientific papers in refereed books, journals, and conference proceedings in his research area. He has served as general chair, programmer chair, and member on scientific and organizing committees of numerous international conferences. He is a member of the editorial board of Cognitive Computation, International Journal of Modelling, Identification and Control, Frontiers in Robotics and AI: Multi-robot systems. He was the chair of Chinese Automation and Computing Society in the UK (2016-2017). He was an IEEE senior member.